Improvement of the fluorescent sensing biomarker 3-nitrotyrosine for a new luminescent coordination polymer by size regulation

Jun Geng, Hongyan Lin, Xiaohui Li, Junjun Lu, Qianqian Liu and Xiuli Wang*

College of Chemistry and Materials Engineering, Professional Technology Innovation Center of Liaoning Province for Conversion Materials of Solar Cell, Bohai University, Jinzhou 121013, P. R. China

Section 1 Experimental

I. Materials and general methods

The ligand L was prepared according to the synthesis method of the literature.[1] The reagents and solvents used in the experiments were purchased from commercial sources and used without further purification. The single X-ray diffraction (XRD) data for LCP **1** was collected by using a Bruker SMART APEX II CCD diffractometer at 293 K with Mo Kα radiation (λ = 0.71073 Å). The infrared (IR) spectra data were gathered on a Varian640 FTIR spectrometer through KBr pellet from 500 cm^{-1} to 4000 cm^{-1} region, and the powder X-ray diffraction (PXRD) patterns were collected on a D/teX Ultra diffractometer with Mo Kα radiation (λ =0.71073 Å). The morphology and structure of the samples were characterized by scanning electron microscopy (SEM, Nova NanoSEM 430). The fluorescent spectra were recorded on a Hitachi F-4500 luminescence/phosphorescence spectrometer. Fluorescence lifetime data was obtained on the FLS1000 transient steady-state fluorescence spectrometer. UV-vis absorption spectra were carried out on SP-1900. The PHS-3C-meter with an E-201-C glass electrode was used to determine the pH of the solution.

II. X-ray crystallography.

Data collection was performed on a Bruker Smart APEX II diffractometer with Kα (λ = 0.71073 Å) by θ and ω scan mode at room temperature. The crystal structure was solved by direct method using the SHELXT program of the Olex 2 crystallographic software package and refined on F^2 by full-matrix least-squares methods.[2] Anisotropic thermal parameters were utilized in all non-hydrogen atoms. Crystal data and structural refinements were displayed in Table S1. CCDC No. 2164207. Selected bond lengths

and angles were shown in Table S2 for LCP **1**.

III. Luminescent sensing experiments

During the sensing experiments, LCP **1** (3 mg) was ground in air, dispersed in 4 mL of water or organic solution, and sonicated for 30 min to form a dispersed solution. The Nano-LCP **1** does not need to be ground, other steps are the same as LCP **1**. Then, the analyte to be tested is added to the suspension to perform a fluorescence titration experiments, and the fluorescence intensity is detected by a fluorescence spectrometer. In the cycling experiments, the samples were washed with ethanol, and after drying, the above experimental steps were repeated to continue the fluorescence titration experiments.

Table S1. Crystallographic data for LCP **1**.

Complex	LCP **1**
Empirical formula	$C_{44}H_{34}Cd_3N_4O_{18}$
Formula weight	1243.95
Temperature/K	296.15
Crystal system	triclinic
Space group	*P–1*
a (Å)	9.7026(12)
b (Å)	9.9293(13)
c (Å)	12.8415(16)
α (°)	100.645(2)
β (°)	99.837(2)
γ (°)	116.544(2)
V (Å ^{3})	1041.5(2)
Z	1
D_c (g cm^{-3})	1.983
μ (mm^{-1})	1.606
F (000)	614.0
Reflections collected	5766

Data/restraints/parameters	3671/3/313
Goodness-of-fit on F^2	1.037
Final R indexes [I>=2σ (I)]	$R_1 = 0.0501$, $wR_2 = 0.1202$
Final R indexes [all data]	$R_1 = 0.0844$, $wR_2 = 0.1373$

[a] $R_1 = \Sigma||F_o|-|F_c||/\Sigma|F_o|$, [b] $wR_2 = \Sigma[w(F_o^2-F_c^2)^2]/\Sigma[w(F_o^2)^2]^{1/2}$

Table S2. Selected bond distances (Å) and angles (°) for LCP **1**.

LCP **1**			
Cd(1)-O(5)#1	2.280(5)	O(4)#2-Cd(2)-O(4)	180.0
Cd(1)-O(2)	2.222(6)	O(4)#2-Cd(2)-O(6)#3	86.8(2)
Cd(1)-O(3)	2.445(6)	O(4)-Cd(2)-O(6)#3	93.2(2)
Cd(1)-N(1)	2.296(7)	O(4)#2-Cd(2)-O(6)#4	93.2(2)
Cd(2)-O(4)	2.170(5)	O(4)-Cd(2)-O(6)#4	86.8(2)
Cd(2)-O(4)#2	2.170(5)	O(4)-Cd(2)-O(3)#5	86.7(2)
Cd(2)-O(6)#3	2.310(5)	O(4)#2-Cd(2)-O(3)#5	93.3(2)
Cd(2)-O(6)#4	2.310(5)	O(4)#2-Cd(2)-O(3)#6	86.7(2)
Cd(2)-O(3)#5	2.519(6)	O(4)-Cd(2)-O(3)#6	93.3(2)
Cd(2)-O(3)#6	2.519(6)	O(6)#3-Cd(2)-O(6)#4	180.0
O(5)#1-Cd(1)-O(3)	78.7(2)	O(6)#3-Cd(2)-O(3)#6	104.47(19)
O(5)#1-Cd(1)-N(1)	83.7(2)	O(6)#3-Cd(2)-O(3)#5	75.53(19)
O(2)-Cd(1)-O(5)#1	135.0(2)	O(6)#4-Cd(2)-O(3)#6	75.53(19)
O(2)-Cd(1)-O(3)	92.3(2)	O(6)#4-Cd(2)-O(3)#5	104.47(19)
O(2)-Cd(1)-N(1)	103.2(3)	O(3)#5-Cd(2)-O(3)#6	180
N(1)-Cd(1)-O(3)	161.9(2)		

Symmetry code: #1 –1+X, –1+Y, +Z; #2 3–X,2–Y, –Z; #3 2–X, 2–Y, 2–Z; #4 1+X, +Y, +Z; #5 2–X, 1–Y, 2–Z; #6 1+X, 1+Y, +Z;

Section 2 Results and Discussion

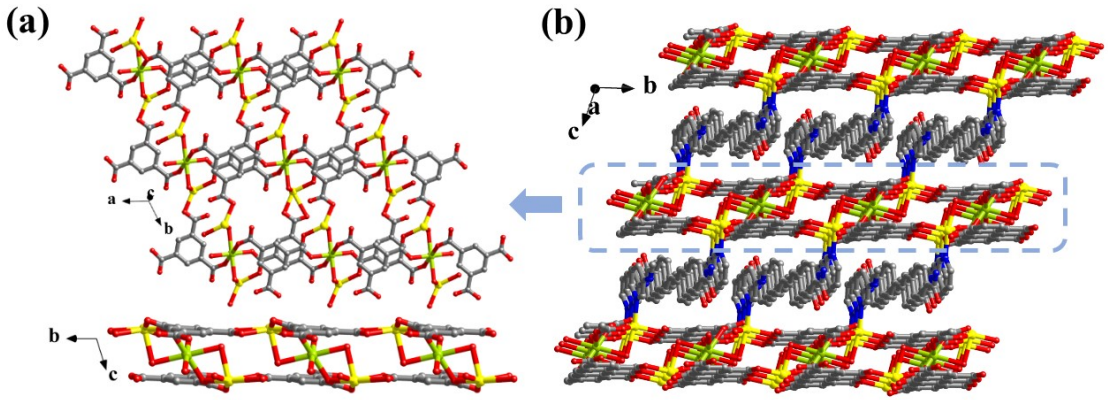

Figure S1. (a) The 2D bilayer structure; (b) View of the 3D framework of LCP **1**.

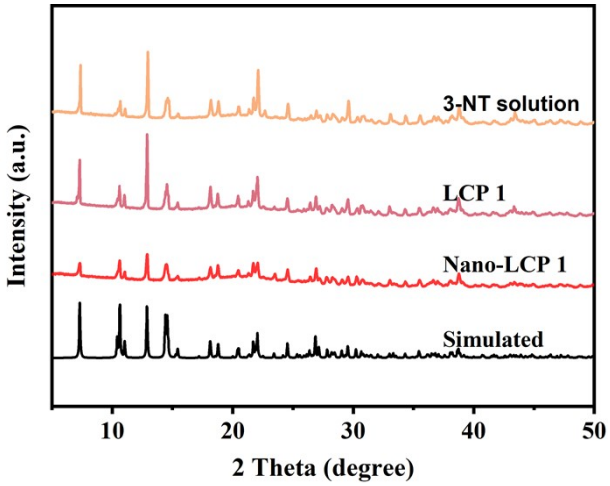

Figure S2. The PXRD of LCP **1** and Nano-LCP **1**.

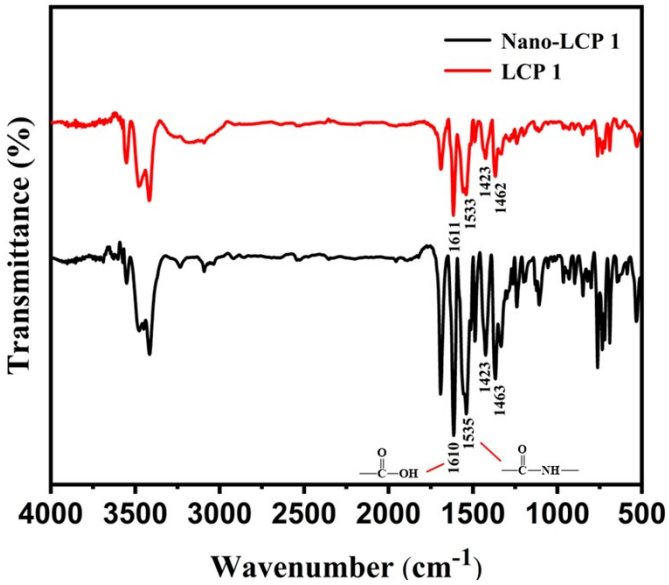

Figure S3. FT-IR spectra of LCP **1** and Nano-LCP **1**.

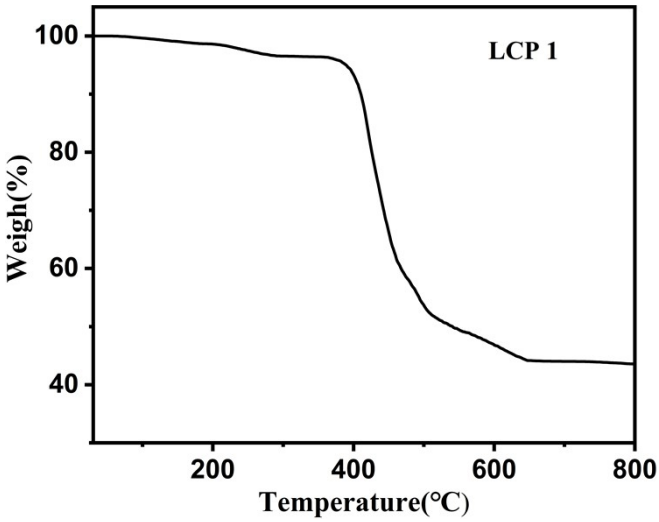

Figure S4. The TG curve of LCP **1**.

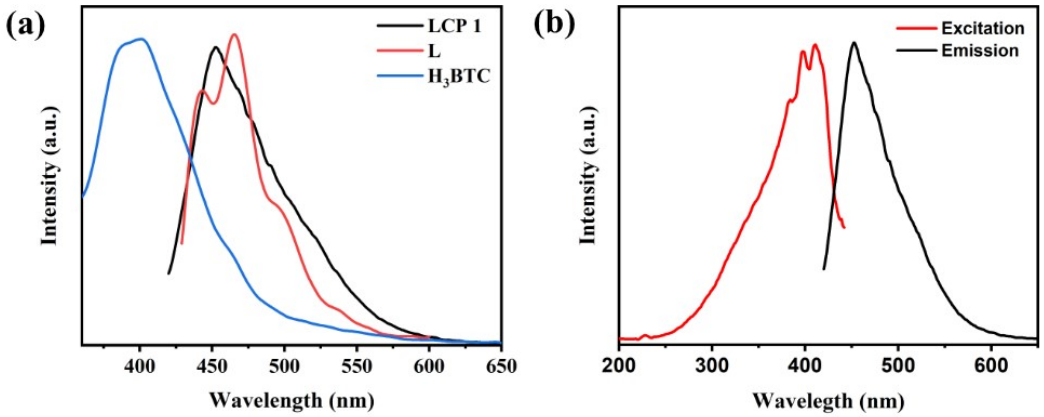

Figure S5. (a) The emission spectra of solid-state LCP **1**, L and H_3BTC; (b) The solid excitation and emission spectra of LCP **1**.

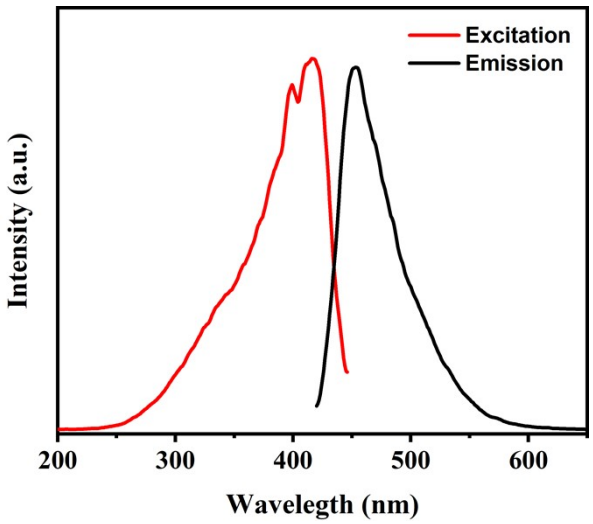

Figure S6. The emission and excitation spectra of solid-state Nano-LCP **1**.

Table S3 Comparison of various methods for 3-NT detection.

Methods	LOD (mol/L)	References
LC-MS/MS	1.70×10^{-11}	Göen et al. (2005)[3]
SPE[a] − HPLC	3.10×10^{-6}	Mergola et al. (2013)[4]
Real time-tandem mass spectrometry	8.80×10^{-7}	Song et al. (2015)[5]
HPLC	2.30×10^{-8}	Monica et al. (2017)[6]
Surface plasmon resonance	5.30×10^{-10}	He et al. (2019)[7]
Molecular Imprinting	2.23×10^{-8}	Martins et al. (2020)[8]
Electrochemiluminescence	8.40×10^{-9}	Zhu et al. (2021)[9]
Fluorescence	3.10×10^{-7}	Wang et al. (2022)[10]
Fluorescence	2.30×10^{-8}	Present work

[a] Solid-phase extraction.

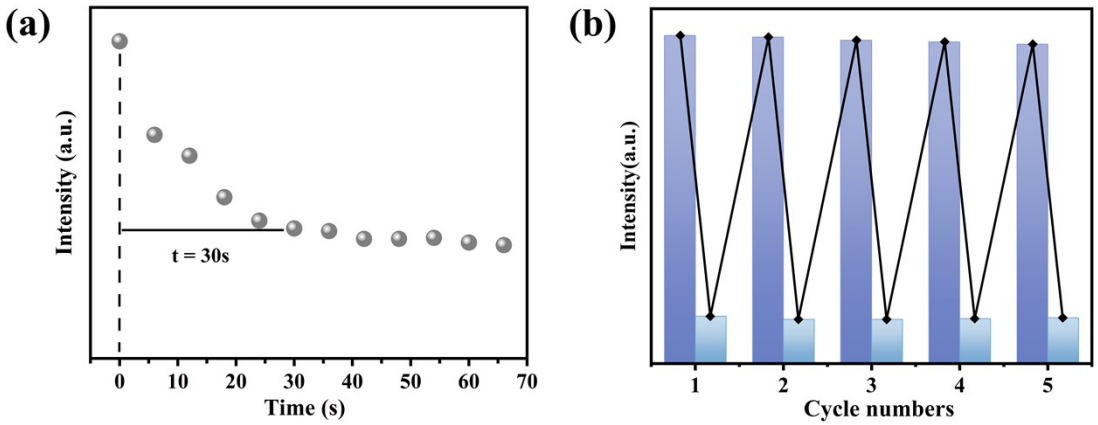

Figure S7. (a) Response time of LCP **1** for 3-NT; (b) Reproducibility of the sensing function of LCP **1** with five continuously quenching cycles (the blue-violet bars are for the luminescence intensity of LCP **1** and the dusty blue bars are for the intensity upon the addition of 3-NT aqueous solution).

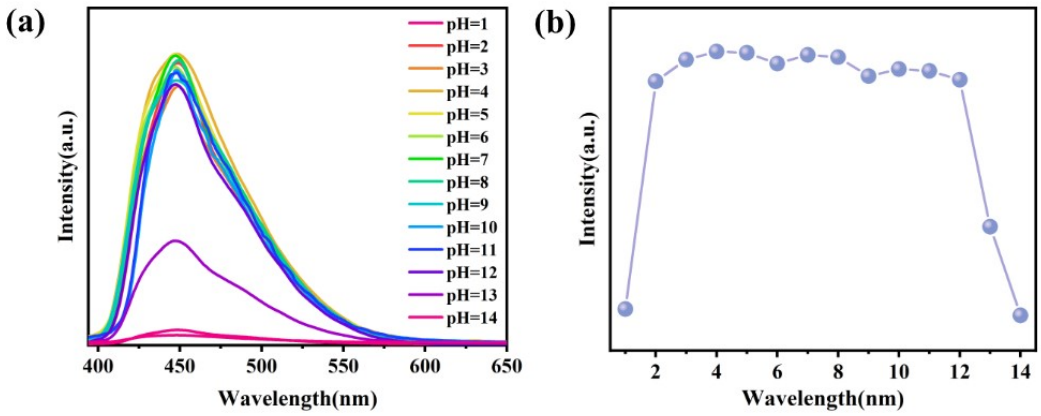

Figure S8. (a) Emission spectra and intensities of LCP **1** suspensions in different pH values; (b) Emission intensity line chart of LCP **1** suspensions in different pH values.

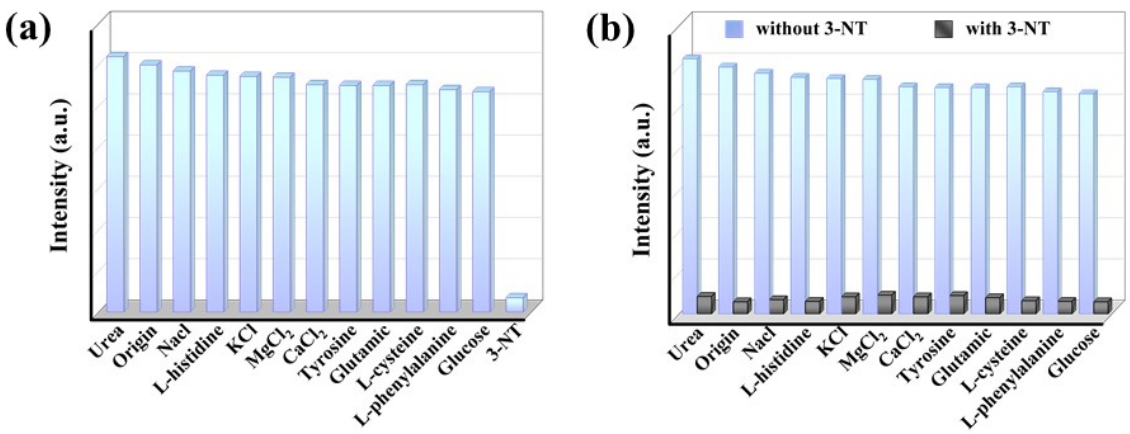

Figure S9. (a) Sensing selectivity of 3-NT by LCP **1** toward the main chemical components in human blood; (b) Anti-interference test of LCP **1** after adding 3-NT in different main chemical components.

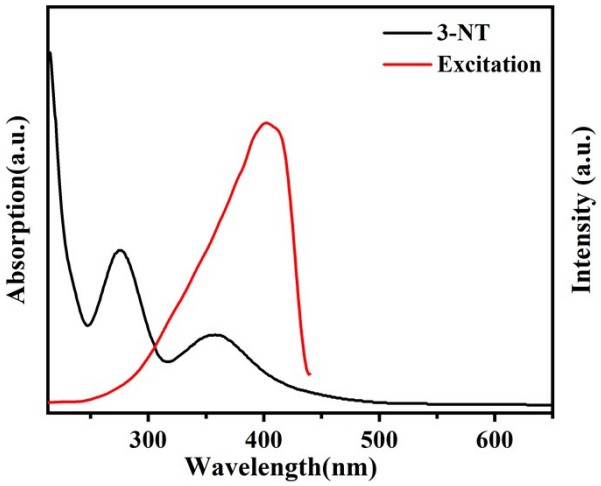

Figure S10. The UV−vis absorption spectra of 3-NT and excitation spectra of LCP **1** in water.

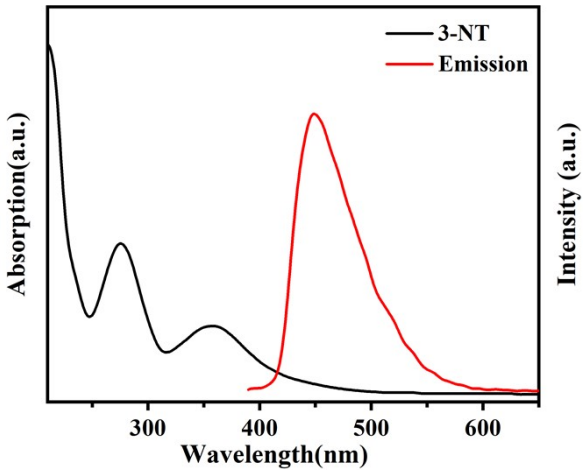

Figure S11. The UV−vis absorption spectra of 3-NT and emission spectra of LCP **1** in water.

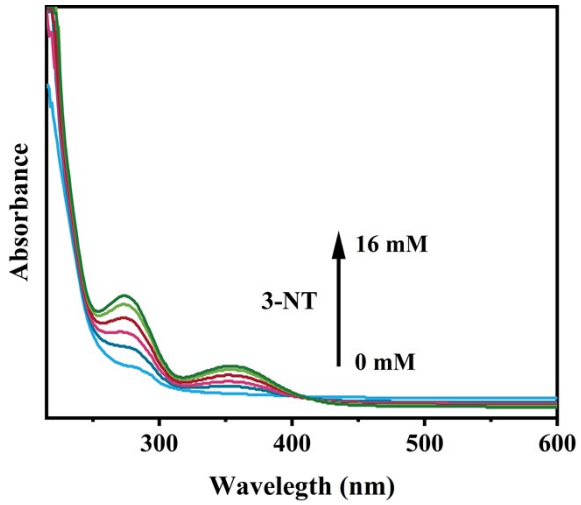

Figure S12. UV−vis spectra of LCP **1** in the presence of various concentrations (0-16 mM) of 3-NT solution.

Table S4. HOMO and LUMO energies calculated for ligand L and analyte at B3LYP/6-31G(d)

	HOMO (eV)	LUMO (eV)	Band Gap (eV)
L	−6.1293	−2.2503	3.8790
3-NT	−6.5713	−2.7987	3.7726

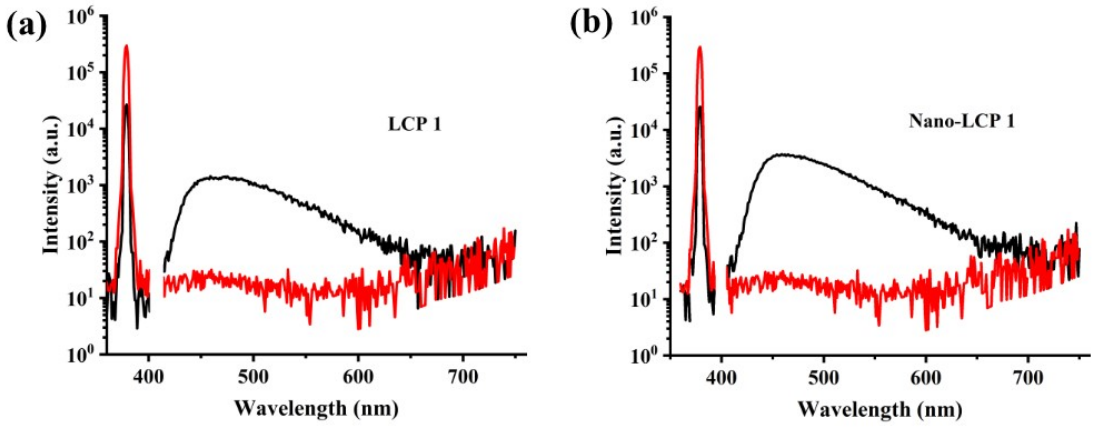

Figure S13. (a) Solid-state quantum yield diagram of LCP **1**; (b) Solid-state quantum yield diagram of Nano-LCP **1**

Table S5. Solid-state quantum yields of LCP **1** and Nano-LCP **1**

	Quantum yield(%)
LCP **1**	13.10%
Nano-LCP **1**	31.80%

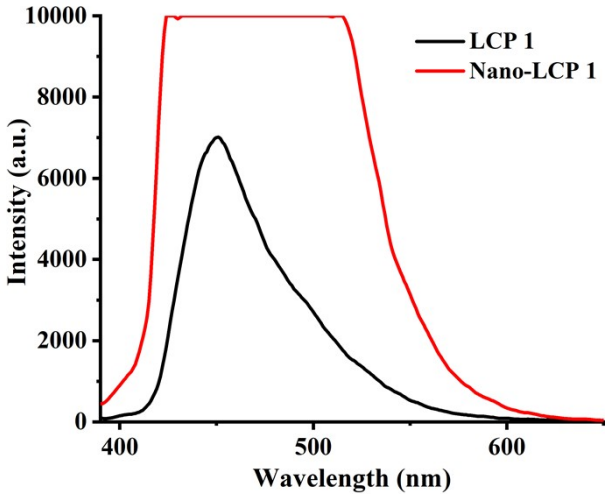

Figure S14. The emission spectra of LCP **1** and Nano-LCP **1**.

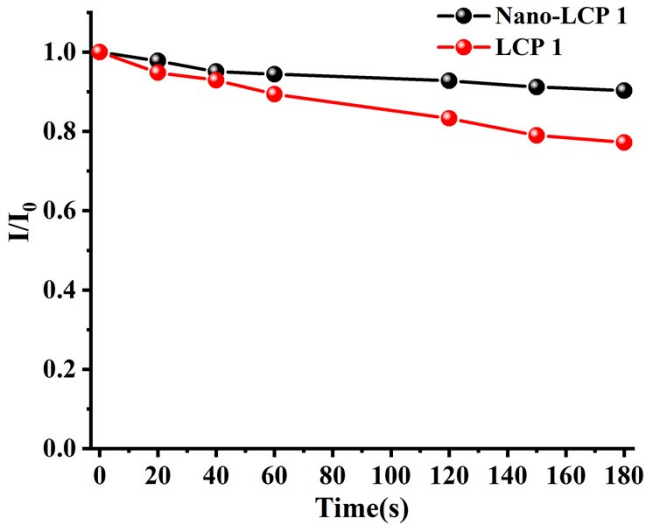

Figure S15. Fluorescence intensity ratio of the LCP **1** and Nano-LCP **1** samples standing within 3 min.

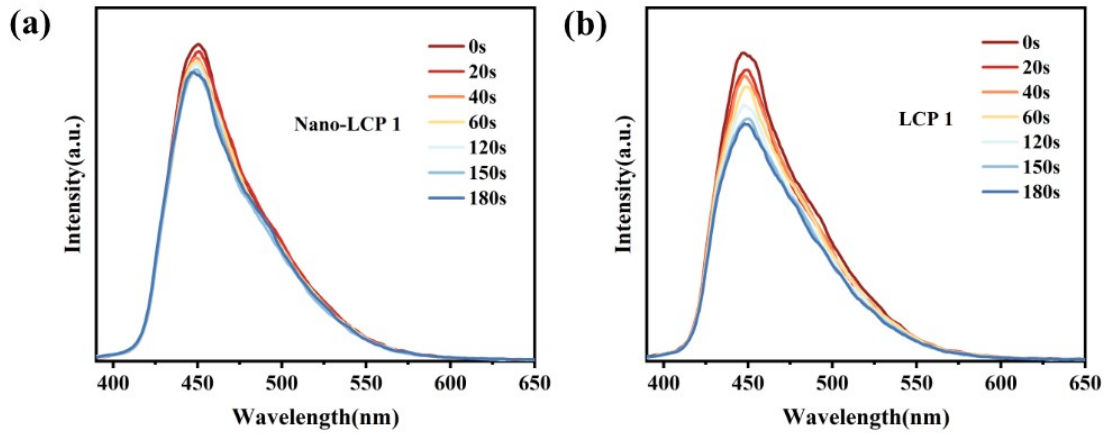

Figure S16. (a-b) Fluorescence intensity of the Nano-LCP **1** and LCP **1** standing within 3 min.

References

1. Y.-F. Hsu, C.-H. Lin, J.-D. Chen and J.-C. Wang, *Cryst. Growth Des.*, 2008, **8**, 2047-2047.
2. G. Sheldrick, *Acta Crystallographica Section A*, 2008, **64**, 112-122.
3. T. Göen, A. Müller-Lux, P. Dewes, A. Musiol and T. Kraus, *J. Chromatogr. B*, 2005, **826**, 261-266.
4. L. Mergola, S. Scorrano, R. Del Sole, M. R. Lazzoi and G. Vasapollo, *Biosens. Bioelectron.*, 2013, **40**, 336-341.
5. Y. Q. Song, J. Liao, C. Zha, B. Wang and C. C. Liu, *Acta Pharm Sin B*, 2015, **5**, 482-486.
6. D. Teixeira, C. Prudencio and M. Vieira, *J. Chromatogr. B Anal. Technol. Biomed. Life Sci.*, 2017, **1046**, 48-57.
7. Q. Y. He, Y. S. Chen, D. Shen, X. P. Cui, C. G. Zhang, H. Y. Yang, W. Y. Zhong, S. A. Eremin, Y. X. Fang and S. Q. Zhao, *Talanta*, 2019, **195**, 655-661.
8. G. V. Martins, A. C. Marques, E. Fortunato and M. G. F. Sales, *Sensing and Bio-Sensing Research*, 2020, **28**, 100333.
9. L. H. Zhu, S. Li, W. X. Liu, J. Chen, Q. W. Yu, Z. Zhang, Y. Li, J. Liu and X. Chen, *Biosens. Bioelectron.*, 2021, **187**, 113284.
10. J. Geng, Y. Y. Li, H. Y. Lin, Q. Q. Liu, J. J. Lu and X. L. Wang, *Dalton Trans.*, 2022, **51**, 11390-11396.